

Methanol Oxidation on a Copper Catalyst Investigated Using in Situ X-ray Photoelectron Spectroscopy[†]

Hendrik Bluhm,^{*,‡} Michael Hävecker, Axel Knop-Gericke, Evgueni Kleimenov, and Robert Schlögl

Abteilung Anorganische Chemie, Fritz-Haber-Institut der Max-Planck-Gesellschaft, Faradayweg 4-6, D-14195 Berlin, Germany

Detre Teschner[§]

Institute of Isotope & Surface Chemistry, CRC, Hungarian Academy of Sciences, P.O. Box 77, Budapest, H-1525 Hungary

Valerii I. Bukhtiyarov

Boreskov Institute of Catalysis, 6300090 Novosibirsk, Russia

D. Frank Ogletree and Miquel Salmeron

Materials Sciences Division, Lawrence Berkeley National Laboratory, One Cyclotron Road, Berkeley, California 94720

Received: January 28, 2004; In Final Form: March 25, 2004

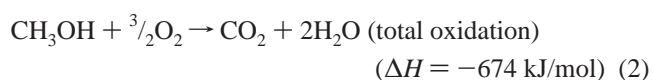
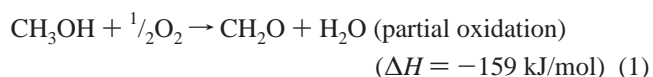
The surface and near-surface regions of an active catalyst and the adjacent gas-phase reactants were investigated simultaneously under reaction conditions using in situ X-ray photoelectron spectroscopy (XPS). This investigation of methanol oxidation on a copper catalyst showed that there was a linear correlation between the catalytic activity of the sample and the presence of a subsurface oxygen species that can only be observed in situ. The concentration profile of the subsurface oxygen species within the first few nanometers below the surface was determined using photon-energy-dependent depth-profiling. The chemical composition of the surface and the near-surface regions varied strongly with the oxygen-to-methanol ratio in the reactant stream. The experiments show that the pure metal is not an active catalyst for the methanol oxidation reaction, but that a certain amount of oxygen has to be present in the subsurface region to activate the catalytic reaction. Oxide formation was found to be detrimental to formaldehyde production. Our results demonstrate also that for an understanding of heterogeneous catalysts a characterization of the surface alone may not be sufficient, and that subsurface characterization is essential.

Introduction

One of the foremost goals of catalytic research is to unravel the atomic-level structure of the catalyst surface and the processes occurring during synthesis operation. Studies under high-vacuum conditions have provided detailed information about the adsorption and stoichiometric reaction of molecules on well-defined surfaces.¹ However, the surface chemistry under those relatively static conditions might be very different from the dynamic surface chemistry at higher pressures.² In the past the in situ investigation of catalyst surfaces was difficult, because the most surface sensitive imaging and spectroscopy techniques were restricted to high-vacuum conditions.^{3,4} Recent instrumental developments, however, have made possible investigations at elevated pressures using imaging^{5–10} and spectroscopic^{11–13} methods, among them X-ray photoelectron spectroscopy (XPS),^{14–16} which has been shown to be able to operate at

pressures of up to 10 mbar.^{17,18} Here we present the use of XPS at millibar pressures to determine the chemical species near the surface of a catalyst, including the gas-phase reaction products, in situ, i.e., while the reaction takes place.

Elemental copper can be used as an unsupported catalyst for the oxidative dehydrogenation of alcohols to their respective aldehydes. In this work the oxidation of methanol is investigated as a model reaction. There are two main reaction paths: partial oxidation to formaldehyde and total oxidation, which is thermodynamically favored:



Room-temperature ultra-high-vacuum (UHV)-XPS studies showed the presence of a methoxy (CH₃O) intermediate at the copper surface.^{19,20} It was found that methanol reacted with preadsorbed oxygen (O_{ads}) on Cu(110) and polycrystalline Cu to methoxy.

[†] Part of the special issue "Gerhard Ertl Festschrift".

^{*} To whom correspondence should be addressed. E-mail: hbluhm@lbl.gov.

[‡] Present address: Chemical Sciences Division, Lawrence Berkeley National Laboratory, Mail Stop 4R0230, Berkeley, CA 94720.

[§] Also at Abteilung Anorganische Chemie, Fritz-Haber-Institut der Max-Planck-Gesellschaft.

The methoxy species then either decomposes to formaldehyde, which desorbs from the surface, or is oxidized to formate (CHOO), which is stable at room temperature, but decomposes at 100 °C to CO₂ and H₂.¹⁹ In situ near-edge X-ray absorption fine structure (NEXAFS) experiments at the oxygen K-edge were performed at temperatures up to 400 °C in different methanol-to-oxygen reactant streams at a total pressure of about 1 mbar.¹² These studies showed that the formaldehyde yield is correlated to the presence of a suboxide species at the sample surface that could only be detected under in situ conditions. The NEXAFS results also showed that the catalytically active phase is metallic. In a recent in situ XPS study of the methanol oxidation on polycrystalline Cu the authors found under reaction conditions an O1s peak at 531 eV, which they ascribed to the suboxide phase.¹⁶ Contrary to the in situ NEXAFS experiments, however, where the formaldehyde yield correlated positively with the abundance of suboxide,¹² the abundance of the 531 eV species in the in situ XPS experiments decreased with increasing formaldehyde yield. This discrepancy might be due to the fact that the in situ NEXAFS measurement in ref 12 were performed under steady-state conditions, while the in situ XPS data in ref 16 were measured during the heating of the sample (0.2 K/min), i.e., not under steady-state conditions.

In the experiments presented in this paper we have used the advantages of synchrotron-based in situ XPS to quantitatively determine the depth-dependent composition of the surface and near-surface regions, to a depth of a few nanometers, during the catalytic reaction. We have also investigated the presence of intermediates of the reaction at the catalytically active surface. From our measurements we will show that there is a correlation between the presence of a subsurface oxygen species and the formation of formaldehyde in the catalytic reaction.

Experimental Section

The experiments were performed at beamline U49/2-PGM1 at BESSY in Berlin,²¹ and at beamline 9.3.2 at the Advanced Light Source in Berkeley.²² The overall spectral resolution was 0.1 eV at the oxygen K-edge. All spectra were normalized by the incident photon flux, which was measured using a photodiode with known quantum efficiency. The methanol vapor and oxygen flows into the experimental cell were regulated using calibrated mass flow controllers. The combined methanol and oxygen pressure in the experimental cell was 0.6 mbar at a total flow rate of ~10 sccm. The sample was a polycrystalline Cu foil (99.99% purity) mounted on a temperature-controlled heating stage.

XPS experiments at elevated pressures face two obstacles: (a) the elastic and inelastic scattering of electrons by gas-phase molecules and (b) the need for high-vacuum conditions for the operation of electron detectors. We have overcome these problems in our experimental setup by using a combination of differential pumping and electrostatic focusing of the emitted photoelectrons.¹⁷ The sample is mounted inside a high-pressure cell 2 mm away from a small aperture (1 mm diameter), which is the entrance to a differentially pumped electrostatic lens system (see Figure 1). Electrons from the sample as well as gas-phase molecules escape through this aperture into the first stage of an electrostatic lens system. The electrons are then subsequently focused onto two more apertures (diameters 2 mm) that are separated by another electrostatic lens unit before they enter the hemispherical analyzer.²³ The combination of electrostatic lenses and differentially pumped apertures allows us to collect electrons with an efficiency similar to that of a conventional hemispherical analyzer, while keeping a pressure

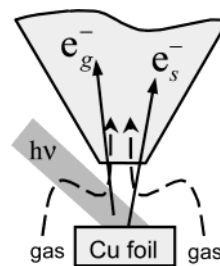


Figure 1. Close-up of the sample–first-aperture geometry. The incident X-rays irradiate the sample under an angle of 55° from the surface normal. The electrons are detected under normal emission. The incident X-rays irradiate not only the sample surface (photoelectrons e_s^-) but also part of the gas phase in front of the sample (photoelectrons e_g^-), which gives rise to gas-phase peaks in the in situ XPS spectra. The aperture diameter was 1 mm and the sample–aperture distance 2 mm.

differential of 9 orders of magnitude between the high-pressure cell and the hemispherical analyzer.

Results and Discussion

We have recorded O1s, valence band, C1s, Cu3p, and Cu2p photoelectron spectra under different conditions: at a fixed methanol-to-oxygen mixing ratio of 3:1 at temperatures from 25 to 450 °C, and at a fixed temperature (400 °C) in varying methanol-to-oxygen mixing ratios. In this paper we present the data of the mixing ratio series.

Figure 2a shows the O1s region of photoemission spectra of the Cu catalyst at an incident photon energy of 720 eV. The four spectra correspond to methanol-to-oxygen mixing ratios in the reactant stream of 1:2, 1:1, 3:1, and 6:1, and a sample temperature of 400 °C. Since the incident X-ray beam irradiates not only the sample surface but also the gas-phase molecules in front of the sample (see Figure 1), the spectra show gas-phase peaks alongside the surface peaks. The binding energy (BE) scale in Figure 2 is referenced to the Fermi level of the Cu sample, and therefore, the apparent BEs of the gas-phase peaks are shifted by the amount of the work function of the sample (~4.5 eV) relative to literature values, which are conventionally referenced to the vacuum level. In Figure 2a peaks with a BE higher than 534 eV are due to gas-phase species, whereas the peaks with a BE smaller than 534 eV are due to oxygen species at the surface. The spectra show a strong dependence on the chemical composition of the reactant stream. Gas-phase peaks of all reactants and products in reactions 1 and 2 (see above) can be distinguished in the spectra. The O₂ gas-phase peaks^{24,25} are strongest for the O₂-rich reaction mixture (CH₃OH:O₂ = 1:2), and weakest for the most methanol-rich mixture (CH₃OH:O₂ = 6:1). The catalytic activity of the copper foil in the four different gas mixtures can be calculated from both the areas of the O1s and C1s peaks and the mass spectrometry data. The results are summarized in Table 1. The absolute amount of formaldehyde produced in the catalytic reaction is highest for the CH₃OH:O₂ = 3:1 mixing ratio.

The key question in catalysis is, of course, how the catalytic reaction depends on the nature of the gas–solid interface, i.e., which species at the catalyst surface are responsible for the catalytic activity. Under our reaction conditions we can distinguish three species at the surface or in the near-surface region under oxidizing (CH₃OH:O₂ = 1:2, 1:1) and two species under reducing (CH₃OH:O₂ = 3:1, 6:1) conditions.

In the CH₃OH:O₂ = 1:2 mixture a peak with a BE of 530.3 eV (fwhm = 1.0 eV) dominated the spectrum. This peak is due to Cu₂O, which was confirmed by comparison to the spectrum of a Cu₂O reference sample that was prepared in a separate

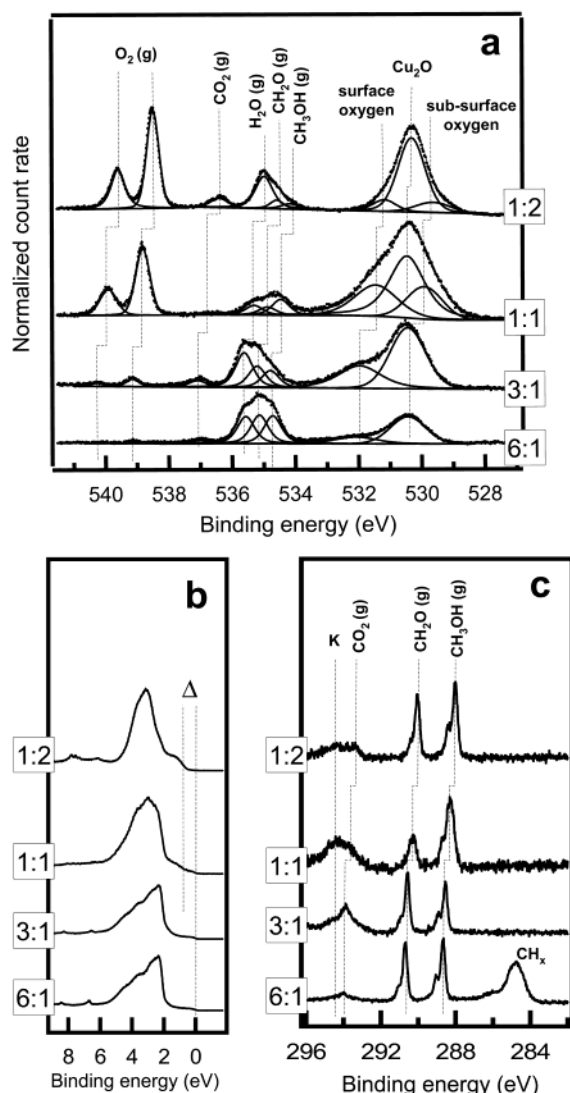


Figure 2. (a) O1s photoelectron spectra of a copper sample at 400 °C in $\text{CH}_3\text{OH}:\text{O}_2$ reactant streams of ratios 1:2, 1:1, 3:1, and 6:1. Raw data are shown as dots, and the results of the fits as solid black lines. The incident photon energy was 720 eV. Gas-phase peaks are found at BEs > 534 eV, and the surface peaks are at BE < 534 eV. In $\text{CH}_3\text{OH}:\text{O}_2 = 1:2$ and 1:1 the Cu_2O peak dominates the surface XPS spectrum. The Cu_2O peak is absent in the spectra that were taken under reducing conditions ($\text{CH}_3\text{OH}:\text{O}_2 = 3:1, 6:1$). In those spectra the subsurface oxygen peak is the strongest peak in the surface part of the spectrum. (b) Corresponding valence band spectra. The spectrum taken in oxidizing conditions ($\text{CH}_3\text{OH}:\text{O}_2 = 1:2$) shows a typical shape for a Cu_2O sample with a gap (Δ) at BE = 0.9 eV, thus confirming the observation from the O1s spectrum in (a). The spectrum taken in $\text{CH}_3\text{OH}:\text{O}_2 = 1:1$ shows that the surface consists of a mixture of metallic copper and Cu_2O . The spectra measured under reducing conditions ($\text{CH}_3\text{OH}:\text{O}_2 = 3:1, 6:1$) exhibit the typical valence band spectrum for metallic Cu, which confirms the absence of a Cu_2O peak in the O1s spectra in (a). (c) C1s spectra taken under the same conditions as in (a) and (b). CO_2 , CH_3OH , and CH_2O gas-phase peaks are observed. There are no carbon-containing species at the surface. Only for $\text{CH}_3\text{OH}:\text{O}_2 = 6:1$ is a peak visible at 284.7 eV, probably due to decomposition products of methanol that accumulate at the surface. The peak at 294.3 eV is due to some potassium contamination.

experiment. The BE of this peak was also in good agreement with literature values for Cu_2O , which vary from 530.2 to 530.5 eV (for a compilation of BE values for the copper oxides see ref 26). In addition, the valence band spectrum taken right after the O1s spectrum (Figure 2b, at a photon energy of 262 eV, i.e., the same probing depth as for the O1s spectra) also shows

TABLE 1: Partial Pressures (mbar) of Methanol, Formaldehyde, and Carbon Dioxide as a Function of the Mixing Ratio of Oxygen and Methanol at 400 °C^a

$\text{CH}_3\text{OH}:\text{O}_2$ mixing ratio	CH_3OH partial pressure	CH_2O partial pressure	CO_2 partial pressure	CH_3OH conversion	CH_2O yield	CO_2 yield
1:2	0.053	0.075	0.072	0.73	0.37	0.36
1:1	0.173	0.070	0.027	0.36	0.26	0.10
3:1	0.167	0.179	0.103	0.63	0.40	0.23
6:1	0.307	0.173	0.030	0.40	0.34	0.06

^a The values are calculated from the gas-phase peak areas measured using XPS. The methanol conversion ($= 1 - (p_{\text{CH}_3\text{OH}}(T)/p_{\text{CH}_3\text{OH}}(25^\circ\text{C}))$), formaldehyde yield ($= p_{\text{CH}_2\text{O}}(T)/p_{\text{CH}_3\text{OH}}(25^\circ\text{C})$), and carbon dioxide yield ($= p_{\text{CO}_2}(T)/p_{\text{CH}_3\text{OH}}(25^\circ\text{C})$) are also given.

a typical Cu_2O spectrum, in agreement with literature spectra²⁶ and our Cu_2O reference spectrum. Two smaller peaks at BEs of 529.7 eV (fwhm = 1.3 eV) and 531.2 eV (fwhm = 1.6 eV) were also present under oxidizing conditions.

When the ratio of methanol to oxygen in the reactant stream was changed to 1:1, the relative intensity of the Cu_2O peak decreased with respect to those of the two other peaks. The binding energies changed to 530.4 eV for the Cu_2O peak, and 529.9 and 531.4 eV for the other two peaks. The valence band spectrum now shows that the surface is covered by both Cu_2O and metallic areas. This is evident from the gap (Δ) at BE = 0.9 eV, which is characteristic for Cu_2O , and the nonzero intensity at the Fermi edge, which is characteristic for a metallic surface. The shape of the spectrum also resembles a mixture of the pure metallic and the pure Cu_2O spectra.

When the sample was measured under reducing conditions ($\text{CH}_3\text{OH}:\text{O}_2 = 3:1, 6:1$), the valence band spectra showed clearly that the surface is metallic, since they exhibited the characteristic spectrum for metallic copper.²⁷ In the O1s region two peaks with BEs of 530.4 and 532.0 eV dominated the spectra. Since the valence band spectra show that the surface is metallic, the peak at 530.4 eV cannot be due to Cu_2O .

We will now turn our attention to the C1s spectra to find out whether the peaks at 530.4 and 532.0 eV in the $\text{CH}_3\text{OH}:\text{O}_2 = 3:1$ and 6:1 O1s spectra are caused by oxygen–carbon compounds. Like the O1s spectra in Figure 2a the C1s spectra in Figure 2c show the gas-phase peaks of CO_2 , CH_2O , and CH_3OH . We do not, however, observe any of the likely intermediates of the methanol oxidation reaction, such as methoxy (BE = 285.2 eV)¹⁹ or formate (BE = 287.7 eV).¹⁹ We also do not observe any other surface carbon species (the BEs of the C1s lines of C–H–O compounds range from 284 to 293 eV).²⁸ Since the elemental detection limit in XPS is on the order of 2%,²⁹ we can conclude that, if intermediates are present at the surface, their concentration must be below that value. Only under the most methanol-rich condition ($\text{CH}_3\text{OH}:\text{O}_2 = 6:1$) is there a peak at 284.7 eV with a smaller shoulder at 286.2 eV. Those peaks are probably caused by decomposition products of methanol on the hot copper surface. From the known O1s/C1s detection sensitivity in our experiment we can estimate that if the 284.7 eV peak were due to a C–O compound with a C:O ratio of 1, its O1s peak would have a peak area similar to that of the 530.4 eV peak in the $\text{CH}_3\text{OH}:\text{O}_2 = 6:1$ O1s spectrum. Since there is no additional peak in the O1s spectrum at 6:1 when compared to the, e.g., 3:1 spectrum, the C1s peaks in the 6:1 spectrum are not likely to be caused by a C–O compound, but rather by some CH_x compound or pure carbon.

In all C1s spectra in Figure 2c some potassium contamination at the surface can be observed ($\text{K}2p_{3/2}$ at 294.3 eV). The

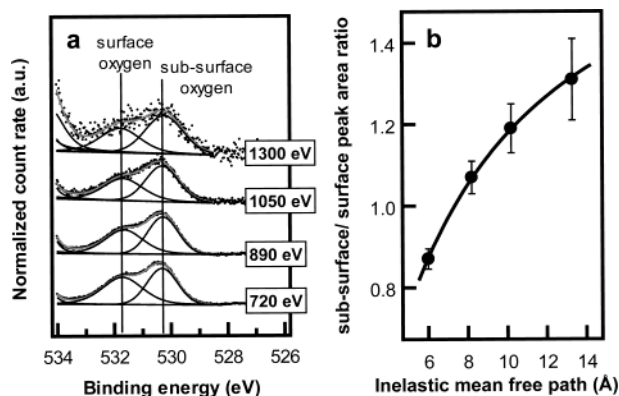


Figure 3. (a) O1s spectra as a function of incident photon energy in $\text{CH}_3\text{OH}:\text{O}_2 = 3:1$ at 400°C . The incident photon energy is indicated for each spectrum. In the fits of the peaks their relative BE position was kept constant, as well as the ratio of their fwhm values. The fwhm ratio was kept constant instead of the absolute values to account for the decrease of the spectral resolution with increasing incident photon energy, which leads to a broadening of the peaks. (b) Peak area ratio of the subsurface oxygen (530.4 eV) and surface oxygen (532.0 eV) O1s peaks calculated from the peak areas in (a). The relative increase of the spectral weight of the 530.4 eV peak with increasing inelastic mean free path indicates that this species is located below the 532.0 eV species, in the subsurface region. The spacing between neighboring atomic layers in Cu in the [100] direction is 1.8 Å . The solid line is a least-squares fit of the data points using $I_{530.4}/I_{532.0} = (n_{530.4}/n_{532.0})\exp[-(z_{532.0} - z_{530.4})/\lambda]$, with I the integrated intensity of the peak, n the concentration in atom percent, z the average depth below the surface, and λ the inelastic mean free path. The fit parameters are $n_{530.4}/n_{532.0} = 1.8$ and $z_{532.0} - z_{530.4} = 4\text{ Å}$.

influence of the K contamination on our results seems to be negligible, since we did not find a correlation of the amount of K at the surface with the catalytic activity. The maximum amount of potassium at the surface was estimated to be $<5\%$ of the total amount of oxygen at all times.

The nature of the O1s peaks at BE = 530.4 and 532.0 eV under reducing conditions (see Figure 2a) was investigated using depth-profiling by variation of the incident photon energy. Because the mean free path of an electron in a solid depends on its kinetic energy (KE), the escape depth of the photoelectrons varies with the incident photon energy ($h\nu$), since $\text{KE} = h\nu - \text{BE} - \Phi$ (where Φ is the work function).³⁰ We have recorded O1s spectra at four different incident photon energies: 720, 890, 1050, and 1300 eV (see Figure 3a). These photon energies correspond to mean free path lengths of 6, 8, 10, and 13 Å, respectively (assuming predominantly copper in the near-surface region).³¹

The depth-profiling measurements revealed that the 532.0 eV peak intensity decreased with respect to the 530.4 eV peak intensity with increasing mean free path length (see Figure 3b). This implies that the 532.0 eV species is located at the surface while the 530.4 eV species extends into the subsurface region. The fit of the data points in Figure 3b yields an *average* separation of 4 Å of the two species in the direction perpendicular to the surface. This average value does not give information about the actual depth distribution of the two species, but it confirms that the 530.4 eV species has to be located below, or at least be embedded in, the surface. The exact nature of the surface peak at 532.0 eV is not clear. Its BE fits that of an OH^- species,³² but it could as well be caused by oxygen bound by residual impurities at the copper surface. It is noteworthy that this peak did not show any correlation to the catalytic activity of the sample, and could also be observed under high-vacuum conditions. A recent in situ XPS study of the

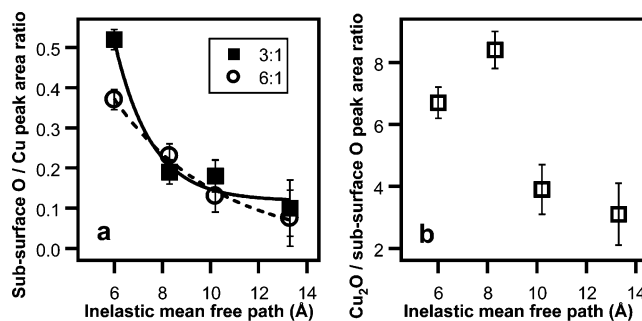


Figure 4. (a) Subsurface O-to-Cu stoichiometry under reducing conditions as a function of the inelastic mean free path of the photoelectrons. The concentration of subsurface oxygen close to the sample surface is higher for the oxygen-rich atmosphere ($\text{CH}_3\text{OH}:\text{O}_2 = 3:1$). Deeper into the sample the concentration of subsurface oxygen is similar for the two different atmospheres. (b) Subsurface oxygen-to- Cu_2O peak area ratio as a function of the inelastic mean free path of the photoelectrons under oxidizing conditions ($\text{CH}_3\text{OH}:\text{O}_2 = 1:2$). Cu_2O is predominantly located at the sample surface.

methanol oxidation on copper also found two peaks at the O1s edge under reaction conditions with BEs similar to those of our surface peaks.¹⁶ The authors of this study assigned the low-BE peak (529.8 eV) to adsorbed oxygen, and the peak at 531.2 eV to a suboxide species. This assignment cannot be made for the peaks in Figure 2a that are observed under reducing conditions, since the depth-profiling data in Figure 3b show that the low-BE species is located below the surface and therefore cannot be adsorbed oxygen.

In the previous discussion we have shown that the peak at 530.4 eV under reducing conditions is due to subsurface oxygen, which could be in the form of a suboxide as discussed in ref 12, oxygen “rafts” below the surface as proposed for the case of Ru,³³ or oxygen located at grain boundaries in the polycrystalline copper sample. The subsurface oxygen peak could only be observed in in situ measurements. When the oxygen flow to the cell was stopped, the subsurface oxygen peak vanished in less than 1 s. We can estimate the average concentration of subsurface oxygen as a function of the depth from the surface. To that end the O1s peak area of the subsurface oxygen peak measured at different photoelectron mean free path lengths was compared to the Cu3p peak area measured at the same mean free path lengths. The BEs of $\text{Cu}3p_{1/2}$ and $\text{Cu}3p_{3/2}$ are 77.3 and 75.1 eV, respectively. Cu3p spectra were taken at incident beam energies of 262, 432, 582, and 842 eV.³⁴ The O:Cu stoichiometry was then calculated from the O1s and Cu3p peak areas at similar KEs, after correction for the energy-dependent changes of the photoemission cross-sections for Cu3p and O1s.³⁵

The results for the active catalyst surface shown in Figure 4a indicate that there is an oxygen concentration gradient perpendicular to the surface. In both reducing gas atmospheres, the concentration of subsurface oxygen is highest close to the surface, and decreases below the surface, which is in agreement with the Δz value from the fit in Figure 3b. At our largest probing depth of 15 Å the Cu:O stoichiometry is about 10, similar to the value found in in situ NEXAFS experiments of the methanol oxidation on a Cu foil under the same reaction conditions.³⁶ Those NEXAFS experiments were performed in the total electron yield detection mode, where the probing depth is estimated to be 20 Å , i.e., similar to the largest probing depth in our experiments.³⁷

It is also noteworthy that in the case of $\text{CH}_3\text{OH}:\text{O}_2 = 3:1$ the O:Cu stoichiometry close to the surface is similar to that of Cu_2O . The valence band spectra in Figure 2b, however, have

shown that even at such an oxygen concentration the sample surface region still has a metallic character. This is also in good agreement with the above-mentioned in situ NEXAFS measurements where the O K-edge and Cu L-edge spectra of the catalytically active surface under reducing conditions showed no resemblance to the spectra of either of the stoichiometric copper oxides Cu_2O and CuO .³⁶

We have also performed depth-profiling on the copper surface under oxidizing conditions ($\text{CH}_3\text{OH}:\text{O}_2 = 1:2$). In Figure 4b the ratio of the peak areas of the peak at 529.7 eV vs the Cu_2O peak is shown. Figure 4b is consistent with a surface mostly covered by a Cu_2O layer with the 529.7 eV oxygen species below. This indicates that the peak at 529.7 eV under oxidizing conditions is most likely also caused by subsurface oxygen, similar to the peak at 530.4 eV under reducing conditions, even though the BEs of the two peaks are different. In other in situ XPS experiments of the methanol oxidation on copper we have observed that the BE of the subsurface species can vary between 529.7 and 530.5 eV, depending on the exposure time of the Cu sample to the reaction mixture and the presence of other oxygen species at the surface. Variations in the faceting of the polycrystalline Cu surface might contribute to the variations in the BE of the subsurface species. The BE of the high-BE surface species in Figure 2a also shifts by about the same amount as that of the subsurface oxygen peak.

From Figure 2a it is evident that the BEs of the gas-phase peaks shift in the same direction as the BEs of the surface peaks on going from oxidizing to reducing conditions. Unlike the shift of the surface peaks, the gas-phase peak shifts are caused by a change of the work function of the sample surface upon reduction. Changes of the sample work function have an influence on the gas-phase peak positions, since the vacuum level of the gas-phase molecules depends on the work function of the surrounding surfaces.³⁸ When a clean metallic Cu surface is oxidized to Cu_2O , its work function increases by about 0.3 eV.^{39,40} An increase in the sample work function increases the kinetic energy of the gas-phase photoelectrons, and therefore decreases their apparent BE when the BE scale is referenced to the Fermi energy of the sample, as is done in our case.⁴¹ The apparent shift of the BE of the gas-phase species in the measurement of the oxidized and the metallic samples in Figure 2a is +0.5 eV, i.e., on the order of the work function change measured during the oxidation of Cu to Cu_2O .

To find a relation between the catalytic activity of the sample and the state of its surface, we have to compare the abundance of the surface species with the formaldehyde yield. Figure 5 shows the dependence of the CH_2O partial pressure on the abundance of subsurface oxygen in the sample (expressed in terms of its peak area) for the four $\text{CH}_3\text{OH}:\text{O}_2$ mixing ratios, and also for a separate experiment where the $\text{CH}_3\text{OH}:\text{O}_2$ mixing ratio was kept constant at 3:1, but the temperature was varied in the range from 150 to 450 °C. There is a linear correlation between the abundance of subsurface oxygen and the yield of CH_2O , in good agreement with in situ NEXAFS data.³⁶ Figure 5 also shows that, in the absence of subsurface oxygen, there is no catalytic activity toward the partial oxidation of methanol.

Having thus proved that the copper catalyst has to contain subsurface oxygen to be active in the partial oxidation of methanol, it remains to be seen what role this species plays in the reaction. Its role could be of a direct nature, for example, by emerging to the surface in a favorable energetic state and geometry, similar to what has been observed in the hydrogenation of ethylene (C_2H_4) on nickel surfaces, where ethylene reacts with subsurface hydrogen to form ethane (C_2H_6).^{2,42,43} Subsur-

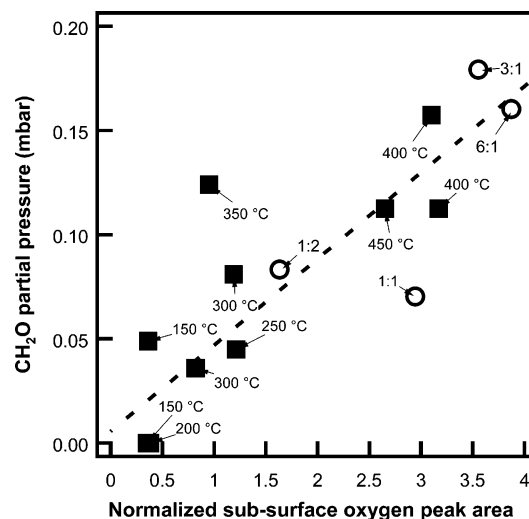


Figure 5. Partial pressure of formaldehyde as a function of the subsurface oxygen peak area for the spectra in Figure 1a (open circles), and for a different experiment (black squares) in which the temperature was varied in the range from 150 to 450 °C at a constant $\text{CH}_3\text{OH}:\text{O}_2$ mixing ratio of 3:1 (the same total pressure as for the spectra in Figure 1a). The partial pressure of formaldehyde is linearly correlated to the abundance of subsurface oxygen in the near-surface region. The dashed line is a linear fit of the data points.

face oxygen could also be indirectly involved in the methanol oxidation, via modification of the copper electronic structure, as shown in recent studies of the methanol synthesis reaction on binary Cu/ZnO catalysts.⁴⁴ In these studies it is argued that strain in the copper surface leads to an increased catalytic activity, as was concluded from density functional calculations that show that strain causes an upshift of the d-band center, which in turn leads to a higher substrate–adsorbate interaction.⁴⁵ The valence band spectra in our experiments do not show systematic variations of the d-band center with the catalytic activity, but the changes that are predicted by the theory are rather small (on the order of 0.1 eV) so that we cannot exclude this explanation for the increased catalytic activity of the copper sample. We propose that the subsurface oxygen species that we find in our catalytically active Cu samples plays the role of a cocatalyst. It is not a reaction partner in the catalytic reaction (unlike O_{ads} in the model discussed in refs 19 and 20), but, together with the neighboring Cu atoms, forms the active center where the reaction takes place.

The presence of oxygen species at and below the Cu surface (as found in our in situ XPS experiments using nondestructive depth-profiling) is also supported by scanning electron microscopy (SEM) investigations of the morphology of Cu foils that were used in atmospheric pressure conversion experiments. At 400 °C in stoichiometric feed ($\text{CH}_3\text{OH}:\text{O}_2 = 2:1$) the Cu foil reached a steady-state performance after 1 h, with 68% CH_3OH conversion and more than 88% selectivity to formaldehyde. No hydrogen was found in the exit stream, in contrast to the Ag system that produces at higher temperatures a significant amount of hydrogen. In Figure 6 characteristic SEM images of a Cu foil that was exposed to He at 400 °C (Figure 6a) and a Cu foil that was exposed to stoichiometric methanol/oxygen feed at 400 °C (Figure 6b) are compared. In both cases significant restructuring and roughening in the submicrometer range has occurred. Using electron backscattering diffraction (EBSD), it was possible to deduce that the preferred surface orientation in the inert gas is [112] (see Figure 6a) whereas it is clearly [111] in oxygen/He (not shown here) and a mixture of the two orientations with a strong predominance of [111] in the feed gas (see Figure 6b).

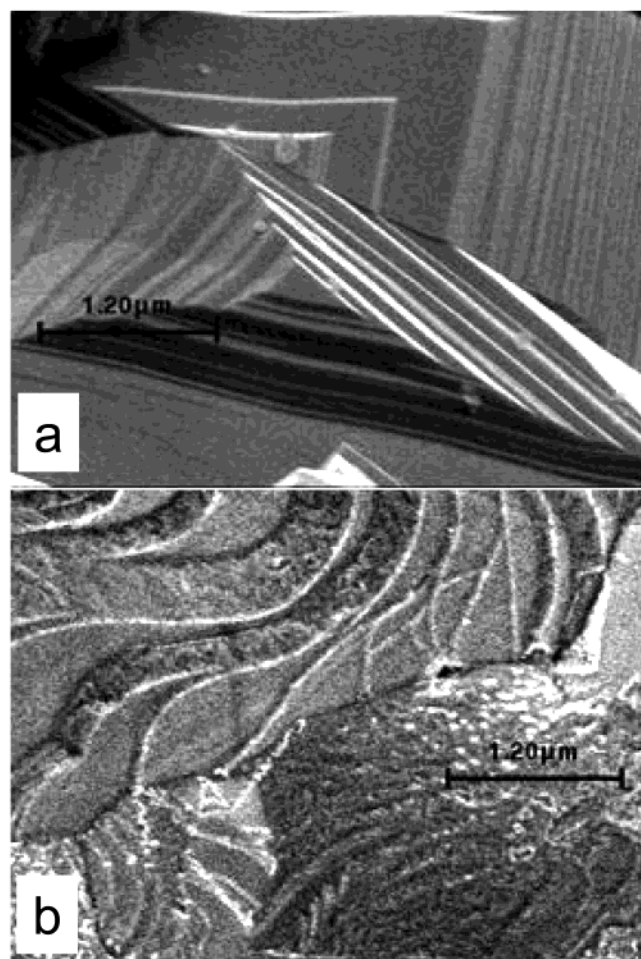


Figure 6. Scanning electron microscopy images of a copper foil that was exposed at 400 °C to (a) helium and (b) a $\text{CH}_3\text{OH}:\text{O}_2 = 2:1$ reactant stream. Whereas the surface that was exposed to helium shows predominantly [112] orientation, the surface that was in the reactant stream exhibits both [112] and [111] domains. Electron backscattering diffraction experiments revealed that the smooth areas in (b) have [111] orientation while the rough ones are [112] oriented. The granular objects are most likely copper oxide particles.

The low-voltage SEM image in Figure 6b gives a clear impression of the surface roughness and anisotropy of the foil that was exposed to the feed gas, where at least two types of surface orientations coexist. The grain boundaries between differently oriented grains in the untreated foil are retained as sharp boundaries between series of facets. From comparison with the EBSD data it is concluded that the smooth parts of the surface have a [111] orientation, whereas the rough parts are [112] oriented. The granular objects in Figure 6b are most likely copper oxides, since the presence of impurities (such as foreign heavy elements) could be ruled out from point energy-dispersive X-ray analysis (EDX) measurements. The presence of oxygen thus has a clear influence on mesoscopic restructuring. From the amount of mass transport that is required to achieve the structuring in Figure 6b it is highly probable that some bulk-dissolved oxygen is involved in the change of the stability of the surface orientation. It should be noted that the size of the small features in Figure 6b is still 2 orders of magnitude larger than the depth of information in our XPS experiments.

We now compare our in situ XPS results with the results of UHV-XPS measurements of the methanol oxidation.^{19,20} In the UHV-XPS experiments at room temperature different Cu surfaces [(110), (111), and polycrystalline Cu] were predosed with oxygen, which dissociated and adsorbed on the surface.

When the oxygen-predosed surface was exposed to methanol, methoxy (the intermediate for formaldehyde formation) was formed on all three surfaces. On Cu(110) and on polycrystalline Cu a subsequent reaction of methoxy to formate could be observed, which is assumed to be the intermediate to the total oxidation to CO_2 . The UHV experiments also showed that formate formation did not occur at Cu(111) surfaces. These findings are in agreement with early low-energy electron diffraction studies that showed that the (110) surface showed a higher reactivity than the (111) surface.^{46,47} From the C1s spectra in Figure 2c it is apparent that the concentration of carbon-containing intermediates of the reaction under our reaction conditions (400 °C vs 25 °C in UHV-XPS studies) has to be below the detection limit of XPS, i.e., below ~2%. This does not mean, however, that methoxy and formate are not possible intermediates under our reaction conditions; if the lifetime of the intermediates at our temperatures is shorter than at room temperature, the concentration of the intermediates at the surface is lower compared to that in the room-temperature UHV-XPS investigations.

In a recent microkinetical investigation of the methanol oxidation on silver, the coverage of silver by methoxy, formate, and O_{ads} was calculated.⁴⁸ For Ag at 400 °C in 0.1 mbar of pure oxygen (comparable to the partial pressure of oxygen in our experiments) the authors found a coverage of ~2% of O_{ads} on Ag, i.e., just at the detection limit of XPS. The authors have also calculated the coverage of Ag by O_{ads} , formate, and methoxy in a gas mixture of 32% CH_3OH , 4.5% O_2 , 11.6% CH_2O , 1.3% CO_2 , 7.4% H_2O , and 6.5% H_2 at a total pressure of 1 atm. It was found that in the temperature range from 100 to 600 °C O_{ads} is the dominating species on the surface, and that its coverage is at least 2 orders of magnitude higher than that of methoxy and formate. Even though our experiments were performed on Cu, and the total pressure was lower than that used in the calculations, the results of the theoretical modeling might explain the absence of methoxy and formate peaks in the C1s spectra in Figure 2c. Under our reaction conditions we do not observe O_{ads} , which has a BE of 529.8 eV on polycrystalline Cu.¹⁹ The peak at 530.4 eV under reducing conditions, which would be the most likely candidate for O_{ads} in our data, is due to subsurface oxygen (see Figure 3). Since O_{ads} is the dominating species according to the microkinetical model calculations, it is unlikely that methoxy or formate species are detected in our experiments.

Our experimental results may further be compared to those of theoretical studies of the location of active oxygen species in various metals. The analogy of Cu to the well-studied silver system⁴⁹ had already been used much earlier.⁵⁰ The quantitative differences in the geometry of adsorbates are explained in these studies by the differences in the local chemical metal–oxygen bonding. In a series of detailed studies of multiple Ag–O configurations^{49,51,52} it is further argued that a general trend in metal oxygen systems exists. On going from low temperatures and high oxygen partial pressures to high temperatures and low oxygen partial pressures, a series of transitions should occur, starting from thick oxides over multiple sandwiches of oxygen–metal–oxygen trilayers to a thin surface oxide with metal termination and finally to a pure metal with surface adsorbates. The relevance of bulk-dissolved or subsurface oxygen species for catalytic functions was ruled out on grounds of energy arguments. The extent to which such a scenario may be extrapolated between the well-studied systems Ag–O and Ru–O^{53,54} may be estimated from the thermodynamic data of the

TABLE 2: Enthalpies of Formation for Solid Phases of Selected Oxides (kJ/mol)

	ΔG_f		
	300 K	500 K	700 K
Ag ₂ O	−11	+2	
Cu ₂ O	−148	−132	−117
CuO	−128	−109	−92
RuO ₂	−252	−217	−194

respective heats of formation at the relevant temperatures and at standard pressure (see Table 2).

The data reveal, in agreement with the discussion in ref 49, that Ag does not form a “thick” oxide at catalytically relevant temperatures whereas the other metals do, depending on the partial pressure of oxygen at a given relevant temperature. We therefore assume that the reaction scenario deduced for Ag is also valid for Cu, taking into consideration that there will always be a tendency to have some oxide present in the system, which is indeed found in the present work.

The data in Figures 2 and 3 imply an agreement with the general scenario, where the oxide-to-metal transition is achieved by the variation of the CH₃OH:O₂ ratio in the feed. This transition is accompanied by a modification of the surface orientation, where a mixture of at least two different terminations with quite different surface structural properties will be present at the surface. Due to this complication it is not possible to quantitatively compare theory and experiment, since the phase diagrams in the literature do not take into account the structure sensitivity of at least the adsorbate phases.

In the case of silver the oxygen-poor phase after the oxide-to-metal transition is a trilayer with oxygen in the hollow sites of a metal terminating layer, and a layer of subsurface oxygen.⁵⁵ An arrangement of two trilayers that are stacked together would fill the depth of information that is accessible in our XPS experiments. What is assigned in the present work as subsurface oxygen may therefore be similar to an arrangement of trilayers in the terminology used in, e.g., ref 53. The approximate stoichiometry of the subsurface species that is found in our work (\sim Cu₂O) would also be consistent with this assignment. Recent in situ NEXAFS experiments¹² showed the same correlation between formaldehyde yield and abundance of a subsurface oxygen species as in our experiments (see Figure 5). From the NEXAFS results we can conclude that the oxygen in these trilayers would have to be differently bonded to copper than in Cu₂O, with a reduced rehybridization between oxygen and copper. It remains speculative in the absence of a theoretical model of this system if oxygen surrounded by metal atoms or the local geometric variation of the metal–metal interaction caused by the presence of the oxygen is the cause for the catalytic activity of the Cu–O trilayer ensemble.

The surface oxygen species in the present work would correlate to the surface adsorbates at undercoordinated metal sites that were identified in the theoretical model of the Ag–O system. This strongly interacting species is not relevant for oxidohydrogenation in the Cu–O system (no correlation of its abundance to catalytic performance in our experiments). The grain boundaries between facets seen in Figure 6 would form typical locations for this species.

From our in situ XPS experiments it follows that the subsurface oxygen species forms with no detectable kinetic hindrance. The oxygen is not desorbing but rather transforming some Cu into oxide species,⁵⁶ similar to the oxide grains in Figure 6b. The shape of the oxygen profiles (see Figure 4) further indicates that there is also a constant abundance of oxygen deeper in the bulk. Such oxygen, deemed not relevant

for catalysis in the theoretical models,⁴⁹ may play a crucial role in the generation and stabilization of the necessary defects that enable a fast interchange of subsurface oxygen among trilayer, adsorbate, and oxide. Its presence would further explain the variation of the peak position of the subsurface species in XPS (see Figure 2), which may be caused by a superposition of the signatures of subsurface and bulk-dissolved species that both do not form strong covalent interactions with the copper d-band.

The experimental observation that all Ag and Cu catalysts require activation under oxidizing conditions and the extensive studies of the deactivation of silver due to an increase of the structural perfection of the metal⁵⁷ support the view that this metastable, bulk-dissolved oxygen has the role of an enabling species for the facile adaptation of the metal–oxygen system to the structures that are dictated by thermodynamics. In this view the observation that a very small average lattice expansion of Cu correlates well with the catalytic activity indicates the importance of lattice defects as “exchange sites” for the surface-to-subsurface migration of oxygen species. Since this lattice expansion is below 0.2%,⁵⁸ it would also explain why we do not observe a shift of the Cu d-band center in our experiments.

Conclusions

Our experiments have shown that the active catalyst surface is metallic copper that contains a subsurface oxygen species. The incorporation of oxygen in the metallic surface will most likely lead to a strained Cu surface lattice. We have also determined that the abundance of subsurface oxygen correlates with the amount of formaldehyde that is produced in the catalytic reaction, and that the pure copper surface would be catalytically inactive in the partial oxidation of methanol to formaldehyde. The truly active surface can only be observed in in situ experiments. Under our experimental conditions (400 °C, $p_{\text{total}} = 0.6$ mbar) we do not observe any intermediates of the reaction. Our experiments have shown not only that the catalytic activity of the copper sample is determined by its surface properties, but that the chemical composition of the subsurface region determines the reactivity of the catalyst.

Acknowledgment. We thank Rolf Follath (Bessy, Berlin) and Ed Wong (ALS, Berkeley) for their help during the measurements. We also thank Gisela Weinberg and Hans-Jörg Wölk (Fritz Haber Institute, Berlin) for providing the SEM images of the Cu foils. Financial support by the German Research Council (DFG) in the framework of the Brücken-schlagsprojekt “Schl. 332/4-1” is gratefully acknowledged. This work was also supported by the Director, Office of Science, Office of Basic Energy Sciences, Division of Materials Sciences and Engineering, U.S. Department of Energy, under Contract No. DE-AC03-76SF00098.

References and Notes

- (1) Somorjai, G. A. *Introduction to Surface Chemistry and Catalysis*; Wiley & Sons: New York, 1994.
- (2) Ceyer, S. T. *Acc. Chem. Res.* **2001**, 34, 737.
- (3) Campbell, C. T. *Science* **2001**, 294, 1471.
- (4) Jaeger, N. I. *Science* **2001**, 293, 1601.
- (5) Sachs, C.; Hillebrand, M.; Völkening, S.; Wintterlin, J.; Ertl, G. *Science* **2001**, 293, 1635.
- (6) McIntyre, B. J.; Salmeron, M.; Somorjai, G. A. *Catal. Lett.* **1992**, 14, 263.
- (7) Hansen, T. W.; Wagner, J. B.; Hansen, P. L.; Dahl, S.; Topsøe, H.; Jacobson, C. J. H. *Science* **2001**, 294, 1508.
- (8) Hansen, P. L.; Wagner, J. B.; Helvig, S.; Rostrup-Nielsen, J. R.; Clausen, B. S.; Topsøe, H. *Science* **2002**, 295, 2053.
- (9) Österlund, L.; Rasmussen, P. B.; Thøstrup, P.; Lægsgaard, E.; Stensgaard, I.; Besenbacher, F. *Phys. Rev. Lett.* **2001**, 86, 460.

- (10) Hendriksen, B. L. M.; Frenken, J. W. M. *Phys. Rev. Lett.* **2002**, 89, 046101.
- (11) Dellwig, T.; Rupprechter, G.; Unterhalt, H.; Freund, H.-J. *Phys. Rev. Lett.* **2000**, 85, 776.
- (12) Knop-Gericke, A.; Hävecker, M.; Schedel-Niedrig, T.; Schlögl, R. *Top. Catal.* **2001**, 15, 27.
- (13) Hess, Ch.; Ozensoy, E.; Goodman, D. W. *J. Phys. Chem. B* **2003**, 107, 2759.
- (14) Joyner, R. W.; Roberts, M. W.; Yates, K. *Surf. Sci.* **1979**, 87, 501.
- (15) Ruppender, H.-J.; Grunze, M.; Kong, C. W.; Wilmers, M. *Surf. Interface Anal.* **1990**, 15, 245.
- (16) Bukhtiyarov, V. I.; Prosvirin, I. P.; Tikhomirov, E. P.; Kaichev, V. V.; Sorokin, A. M.; Evstigneev, V. V. *React. Kinet. Catal. Lett.* **2003**, 79, 181.
- (17) Ogletree, D. F.; Bluhm, H.; Lebedev, G.; Fadley, C. S.; Hussain, Z.; Salmeron, M. *Rev. Sci. Instrum.* **2002**, 73, 3872.
- (18) Bluhm, H.; Ogletree, D. F.; Fadley, C. S.; Hussain, Z.; Salmeron, M. *J. Phys.: Condens. Matter* **2002**, 14, L227.
- (19) Carley, A. F.; Owens, A. W.; Rajumon, M. K.; Roberts, M. W.; Jackson, S. D. *Catal. Lett.* **1996**, 37, 79.
- (20) Bowker, M.; Madix, R. J. *Surf. Sci.* **1980**, 95, 190.
- (21) Sawhney, K. J. S.; Senf, F.; Gudat, W. *Nucl. Instrum. Methods, A* **2001**, 467, 466.
- (22) Hussain, Z.; Huff, W. R. A.; Kellar, S. A.; Moler, E. J.; Heimann, P. A.; McKinney, W.; Padmore, H. A.; Fadley, C. S.; Shirley, D. A. *J. Electron. Spectrosc. Relat. Phenom.* **1996**, 80, 401.
- (23) We have used a modified Phoibos 150 hemispherical analyzer made by SPECS GmbH, Berlin, Germany.
- (24) The oxygen gas-phase peak is split into two separate peaks due to the paramagnetic nature of the O₂ molecule. For a detailed discussion of this effect see ref 25.
- (25) Siegbahn K.; Nordling, C.; Johansson, G.; Hedman, J.; Hedén, P. F.; Hamrin, K.; Gelius, U.; Bergmark, T.; Werme, L. O.; Manne, R.; Baer, Y. *ESCA Applied to Free Molecules*; North-Holland: Amsterdam, 1969; pp 56–60.
- (26) Ghijsen, J.; Tjeng, L. H.; van Elp, J.; Eskes, H.; Westerink, J.; Sawatzky, G. A.; Czyzyk, M. T. *Phys. Rev. B* **1988**, 38, 11322.
- (27) Hüfner, S.; Wertheim, G. K.; Wernick, J. H. *Phys. Rev. B* **1973**, 8, 4511.
- (28) NIST X-ray Photoelectron Spectroscopy Database, Version 3.4 (Web version). <http://srdata.nist.gov/xps/>.
- (29) McIntyre, N. S.; Chan, T. C. In *Practical Surface Analysis. Vol. 1: Auger and X-ray Photoelectron Spectroscopy*, 2nd ed.; Briggs, D., Seah, M. P., Eds.; Wiley & Sons: Chichester, U.K., 1990; p 488.
- (30) Rivière, J. C. In *Practical Surface Analysis. Vol. 1: Auger and X-ray Photoelectron Spectroscopy*, 2nd ed.; Briggs, D., Seah, M. P., Eds.; Wiley & Sons: Chichester, U.K., 1990; p 52.
- (31) Tanuma, S.; Powell, C. J.; Penn, D. R. *Surf. Interface Anal.* **1991**, 17, 911.
- (32) Au, Chak-tong; Breza, J.; Roberts, M. W. *Chem. Phys. Lett.* **1979**, 66, 340.
- (33) Reuter, K.; Ganduglia-Pirovano, M. V.; Stampfl, C.; Scheffler, M. *Phys. Rev. B* **2002**, 65, 165403.
- (34) The gas phase has no influence on the relative detection efficiency of O1s or Cu3p photoelectrons, since we always compare measurements where O1s and Cu3p photoelectrons have the same kinetic energy. On the other hand, the attenuation of the incident photon beam depends on the photon energy, which differs for the Cu3p and O1s spectra. In our experiments the beam travels 2 cm through the gas before it hits the sample. For a gas mixture of CH₃OH:O₂ = 3:1 at a total pressure of 0.6 mbar the transmission of the gas phase varies between 0.980 (at $h\nu = 580$ eV) and 0.998 (at $h\nu = 1300$ eV). (The values were calculated using the web interface of the Center for X-ray Optics at Lawrence Berkeley National Laboratory, Berkeley, CA: http://www-cxro.lbl.gov/optical_constants/gastrn2.html.) The error in the calculation of the depth-dependent Cu:O stoichiometry that is caused by attenuation effects in the gas phase is therefore smaller than 2%, well within the error bars in Figure 4.
- (35) Yeh, J. J.; Lindau, I. *At. Data Nucl. Data Tables* **1985**, 32, 1.
- (36) Hävecker, M.; Knop-Gericke, A.; Schedel-Niedrig, T.; Schlögl, R. *Angew. Chem., Int. Ed.* **1998**, 37, 1939.
- (37) Abate, M.; Goedkoop, J. B.; de Groot, F. M. F.; Grioni, M.; Fuggle, J. C.; Hofmann, S.; Petersen, H.; Sacchi, M. *Surf. Interface Anal.* **1992**, 18, 65.
- (38) Siegbahn, H. *J. Phys. Chem.* **1985**, 89, 897.
- (39) Wagner, L. F.; Spicer, W. E. *Surf. Sci.* **1974**, 46, 301.
- (40) Benndorf, C.; Egert, B.; Keller, G.; Seidel, H.; Thieme, F. *J. Phys. Chem. Solids* **1979**, 40, 877.
- (41) Bluhm, H.; Hävecker, M.; Knop-Gericke, A.; Kleimenov, E.; Teschner, D.; Schlögl, R.; Bukhtiyarov, V. I. Manuscript in preparation.
- (42) Daley, S.; Utz, A.; Trautman, T.; Ceyer, S. T. *J. Am. Chem. Soc.* **1994**, 116, 6001.
- (43) Ledentu, V.; Dong, W.; Sautet, P. *J. Am. Chem. Soc.* **2000**, 122, 1796.
- (44) Günther, M. M.; Ressler, T.; Bems, B.; Büscher, C.; Genger, T.; Hinrichsen, O.; Muhler, M.; Schlögl, R. *Catal. Lett.* **2001**, 71, 37.
- (45) Mavrikakis, M.; Hammer, B.; Nørskov, J. K. *Phys. Rev. Lett.* **1998**, 81, 2819.
- (46) Ertl, G. *Surf. Sci.* **1967**, 6, 208.
- (47) Ertl, G. *Surf. Sci.* **1967**, 7, 309.
- (48) Andreasen, A.; Lynggaard, H.; Stegelmann, C.; Stoltze, P. *Surf. Sci.* **2003**, 544, 5.
- (49) Li, W. X.; Stampfl, C.; Scheffler, M. *Phys. Rev. B* **2003**, 68, 165412.
- (50) Shimizu, T.; Tsukada, M. *Surf. Sci. Lett.* **1993**, 295, L1017.
- (51) Li, W. X.; Stampfl, C.; Scheffler, M. *Phys. Rev. B* **2002**, 65, 075407.
- (52) Li, W. X.; Stampfl, C.; Scheffler, M. *Phys. Rev. Lett.* **2003**, 90, 256102.
- (53) Reuter, K.; Stampfl, C.; Ganduglia-Pirovano, M. V.; Scheffler, M. *Chem. Phys. Lett.* **2002**, 352, 311.
- (54) Stampfl, C.; M. Scheffler, M. *Phys. Rev. B* **1996**, 54, 2868.
- (55) Carlisle, C. I.; Fujimoto, T.; Sim, W. S.; King, D. A. *Surf. Sci.* **2000**, 470, 15.
- (56) Schedel-Niedrig, T.; Neisius, T.; Böttger, I.; Kitzelmann, E.; Weinberg, G.; Demuth, D.; Schlögl, R. *Phys. Chem. Chem. Phys.* **2000**, 2, 2407.
- (57) Meima, G. R.; Knijf, L. M.; van Dillen, A. J.; Geus, J. W.; Bongaarts, J. E.; van Buren, F. R.; Delcour, K. *Catal. Today* **1987**, 1, 117.
- (58) Böttger, I.; Schedel-Niedrig, T.; Timpe, O.; Gottschall, R.; Hävecker, M.; Ressler, T.; Schlögl, R. *Chem.—Eur. J.* **2000**, 6, 1870.